Proceedings of the 17th World Congress
The International Federation of Automatic Control
Seoul, Korea, July 6-11, 2008

Generalized Proportional Integral Control for a Robot with Flexible Finger Gripper ⋆

J. Becedas * **I. Payo** * **V. Feliu** * **H. Sira-Ramírez** **

* *Universidad de Castilla-La Mancha, Av. Camilo José Cela s/n, Ciudad Real, Spain (Tel: 0034 926295300; e-mail: {Jonathan.Becedas, Ismael.Payo, Vicente.Feliu}@uclm.es).*
** *Cinvestav IPN, Av. IPN, No. 2503, Col. San Pedro Zacatenco, AP 14740, 07300 Mexico, D. F., Mexico , (e-mail: hsira@cinvestav.mx)*

Abstract: In this paper a Generalized Proportional Integral output feedback control scheme is proposed for grasping tasks. We have designed a flexible finger gripper mounted at the tip of a rigid arm which can grasp and move objects from a place to other so that a bending force control of the flexible gripper is combined with a position control of the rigid arm. Experiments are presented to verify the goodness of the proposed control law.

1. INTRODUCTION

Since the dawn of robotics, the human being has tried to develop different devices with the desire of creating beings similar to him which can help him in its daily work, carrying out repetitive or dangerous tasks. An important aspect of the human being, in contrast to the most of the living beings, is its ability to manipulate any object with the hands. Scientists have tried to provide to the robots this quality since the beginning of the robotics by developing automatic hands. A review of robotic grasping and contact can be found in Bicchi (2000). The control of forces is an important aspect in these robots in which an object must be manipulated without suffering damages. Thus, a careful analysis of the contact forces between the manipulator and the object must be done in these cases. A literature survey of contact dynamics modeling is presented in Gilardi and Sharf (2002). The use of deformable or flexible robotic fingers (in tasks where there is contact with the environment) improves the limited capabilities of robotic rigid fingers, as shown in a survey of Shimoga (1996). Elasticity of flexible fingers allows a greater adaptability between the manipulator and the object and moreover it avoids damages on the contact surfaces. Many works have been published on the subject of flexible manipulators force control, in the past decades, by using different control techniques, as e.g., optimal control (Matsuno and Kasai (1998)), hybrid position/force control (Chiou and Shahinpoor (1988)), frequency domain control techniques (Chapnik et al. (1993)), neural networks (Tian et al. (2004)) or fuzzy logic (Shi and Trabia (2005)). These works deal with the force control of flexible arms and we are interested in a specific application: the use of controlled flexible fingers for grasping tasks. There are some researchers who have also used flexible fingers to grasp objects. Fukuda et al. (1986) designed an adaptive force control for a pair of gripper tips made of aluminium boards sensored with strain gages and actuated by a DC motor. Gorce and Fontaine (1996) carried out a methodology for designing flexible grippers. Tanaka et al. (1996) dealt with the force control of a flexible finger using a piezoelectric as actuator and force sensors distributed along a flexible finger. Linear control (PID) and optimal control (H_∞) are compared with each other. Choi and Cho (2002) used shape memory alloy (SMA) to actuate upon a flexible gripper implementing a H_∞ controller but the response force of the SMA actuator is relatively slow and its applications are limited.

In this paper, a flexible finger gripper (controlling grasping force) mounted at the tip of a rigid arm (controlling tip position) is designed. In the scientific literature there are also some applications in which the manipulator combines rigid and flexible parts, as e.g., Lew and Book (1993) and Yoshikawa et al. (1996) who design a hybrid position/force control of a combined flexible-macro/rigid-micro manipulator system. They use rigid arms to manipulate the object and this presents some disadvantages: fragile objects can be damaged because of the high rigidity and inertia of the rigid part; force sensors are placed at the end-effector, which can be damaged at the collision instant since the contact surface is the sensor. We deal with this limitations and solve the problem by using the rigid part to position the manipulator, because rigid robots are extensively used in the industry, and by designing a flexible finger gripper to manipulate the object, which can be coupled in whatever rigid manipulator. Furthermore, the flexible finger gripper presents the advantages: on the one hand, the sensor is located at the root of the flexible finger, thus the object and the sensor are not damaged in the collision. On the other hand, the high flexibility with an appropriate contact detection algorithm avoid damages on both the object and the manipulator. We have designed a feedback control law based on Generalized Proportional Integral Control (Becedas et al. (2007)), which is found to be robust with respect to the effects of the unknown Coulomb friction in the motor dynamics. This control law has been applied for both rigid and flexible parts of the manipulator. The dynamic model of the flexible finger is based on a lumped-mass model and the force control law only uses feedback from the coupling torque at the root of the flexible finger. Encoder of the flexible finger motor and force sensors placed between the impact surfaces are not required.

This paper is organized as follows: Section 2 describes the dynamic models for both the flexible finger gripper and the

⋆ This research was supported by the Junta de Comunidades de Castilla-La Mancha via project ref.:PBI-05-057 and European Social Fund. and by the Spanish Ministerio de Educacin y Ciencia via project ref.: DPI2006-13834.

rigid arm. Section 3 shows the control law used. In Section 4 experimental results validate the proposed method. Finally, Section 5 describes the main conclusions of this work.

2. MODEL DESCRIPTION

We consider a flexible finger gripper mounted at the tip of a rigid arm as shown in Fig. 1. This gripper should grasp objects with a controlled torque. We shall now study the dynamic model of the flexible finger gripper and the dynamic model of the rigid arm separately.

2.1 Flexible finger gripper

The flexible finger is a lightweight flexible beam actuated by a DC motor. First, we analyze the motor dynamics. After that, we study the flexible finger dynamics and we then combine both.

Motor dynamics – We use a gear DC motor which is supplied by a current servo-amplifier. This servo-amplifier controls the input current to the motor by means of an internally PI current controller and this electrical dynamics can be rejected because this is faster than the mechanical dynamics of the motor. Thus, the servo-amplifier can be considered as a constant relation k_a between the motor current and the voltage supplied to the servo-amplifier by the computer. Fig 2 displays a block diagram of the set-up (servo-amplifier + motor + gear) whose equations are:

$$Motor: \quad k_m i = J\ddot{\hat{\theta}}_m + \nu\dot{\hat{\theta}}_m + \hat{\Gamma}_{Coul} + \hat{\Gamma} \tag{1}$$

$$Servo-amplifier: \quad i = k_a u \tag{2}$$

$$Gear: \quad \hat{\theta}_m = \theta_m n;\ \hat{\Gamma} = \Gamma/n \tag{3}$$

where k_m is the electromechanical constant of the motor, i is the current supplied to the motor by the servo-amplifier, J is the motor inertia, ν is the viscous friction of the motor, $\hat{\Gamma}_{Coul}$ is the unknown Coulomb friction torque, u is the voltage supplied to the servo-amplifier generated by the computer, k_a is the amplifier gain and n is the reduction ratio of the gear [1]. By combining (1), (2) and (3) we obtain the following equation:

$$ku = J\ddot{\hat{\theta}}_m + \nu\dot{\hat{\theta}}_m + \hat{\Gamma}_{Coul} + \frac{\Gamma}{n} \tag{4}$$

where $k = k_m k_a$. The Coulomb friction torque is a nonlinear term in (4) which makes it difficult the study of the motor dynamic model. We assume the following equations for the Coulomb friction torque model:

$$\hat{\Gamma}_{Coul} = \begin{cases} \hat{\Gamma}_C sign(\dot{\hat{\theta}}_m), & |\dot{\hat{\theta}}_m| > 0; \\ \hat{\Gamma}_C sign(u), & |\dot{\hat{\theta}}_m| = 0 \quad \& \quad |u| > 0. \end{cases} \tag{5}$$

where $\hat{\Gamma}_C$ is an unknown constant value which is different for each motor. This nonlinear friction is considered as an input perturbation to the system. As done in Feliu and Ramos (2005), the coupling torque can be canceled in the motor by means of a compensation term. In this case, the voltage supplied to the servo-amplifier is of the form:

$$u = u_c + \frac{\Gamma}{kn} \tag{6}$$

where u_c is the voltage applied before the compensation term as is shown in Fig. 3. Taking this into account, the system (4) is then given by:

$$A_1 u_c = \ddot{\theta}_m + B_1\dot{\theta}_m + \xi_0 \tag{7}$$

where $A_1 = \frac{k}{Jn}$, $B_1 = \frac{\nu}{J}$ and $\xi_0 = \frac{\hat{\Gamma}_{Coul}}{Jn}$ is the disturbance owing to the Coulomb friction.

[1] Note that the magnitudes seen from the motor side of the gear are written with an upper hat and the magnitudes seen from the other side of the gear are written with standard letters.

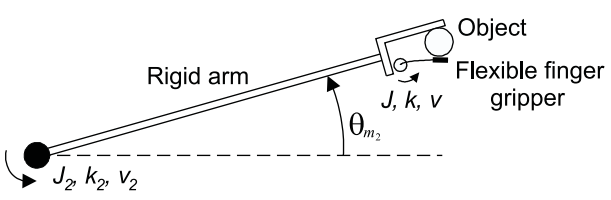

Fig. 1. Flexible finger gripper mounted at the tip of a rigid arm.

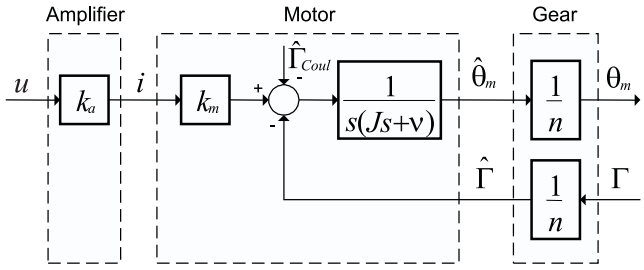

Fig. 2. Block diagram of the servo-amplifier, motor and gear.

Flexible finger dynamics – We consider a lightweight single-link flexible arm of one degree of freedom which is in contact with a rigid body as shown in Fig. 4(a). This arm is actuated by a DC motor in a horizontal plane and is not affected by the gravity effect. We assume that all its mass is concentrated at the tip and small deformations are also considered (see Feliu and Ramos (2005)). The collision is modeled as a spring-dashpot model, Erickson et al. (2003) (see Fig. 4(b)). By considering the separation of the dynamics of the motor and the arm, by means of a compensation of the coupling torque (6) and taking into account the environment impedance, the dynamic model of the flexible arm in contact with an object can be expressed as follows:

$$ml^2\Delta\ddot{\theta}_t + c_e l^2\Delta\dot{\theta}_t + k_e l^2\Delta\theta_t = \Gamma \tag{8}$$

$$\Gamma = c(\theta_m - \theta_t) \tag{9}$$

$$\Delta\theta_t = \theta_t - \theta_e \tag{10}$$

where m is the tip mass, l is the length of the arm, k_e and c_e are the stiffness and damping characteristics of the environment respectively, Γ is the coupling torque, $c = \frac{3EI}{l}$ is the rotational stiffness of the arm, θ_t is the angular position of the arm tip and θ_e is the equilibrium angular position of the impact surface at the moment of the collision. In this manner, $\Delta\theta_t$ is the variation of θ_t with respect to θ_e and thus, $\Delta\dot{\theta}_t \equiv \dot{\theta}_t$ and $\Delta\ddot{\theta}_t \equiv \ddot{\theta}_t$ are the velocity and acceleration of θ_t respectively, since θ_e is a constant value. Taking this into account, the system defined by the expressions (8), (9) and (10) can be written as:

$$M\ddot{\theta}_t + C_e\dot{\theta}_t + K_e\theta_t - K_e\theta_e = \Gamma \tag{11}$$

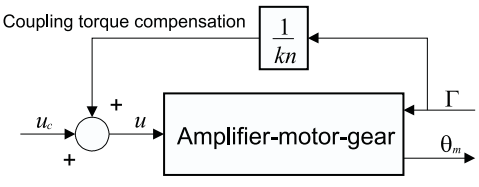

Fig. 3. Compensation of the coupling torque measured in the hub.

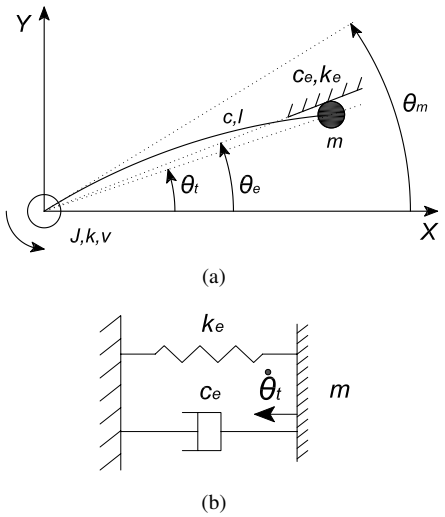

Fig. 4. (a) Scheme of the constrained flexible arm. (b) Collision model.

$$\Gamma = c(\theta_m - \theta_t) \tag{12}$$

where $M = ml^2$, $K_e = k_e l^2$ and $C_e = c_e l^2$. Note that $K_e\theta_e$ is a constant term and this can be considered as a perturbation in the system. By neglecting this term, we can obtain a perturbation free system, in Laplace terms:

$$\theta_t(s)(Ms^2 + C_e s + K_e) = \Gamma(s) \tag{13}$$

$$\Gamma(s) = c(\theta_m(s) - \theta_t(s)) \tag{14}$$

From above expression, the relation between the coupling torque and the motor angle is:

$$\frac{\Gamma(s)}{\theta_m(s)} = \frac{c(s^2 + \frac{C_e}{M}s + \frac{K_e}{M})}{s^2 + \frac{C_e}{M}s + \frac{K_e + c}{M}} \tag{15}$$

If we assume a collision with a rigid object, the constants K_e and C_e are high values, owing to the large values of the environment characteristics k_e and c_e. Therefore, the contact dynamics of the flexible arm with a rigid object is obtained by calculating the following limit of the expression in (15):

$$\lim_{K_e, C_e \to \infty} \frac{\Gamma(s)}{\theta_m(s)} = c \tag{16}$$

Complete system – From (16) we obtain the angular velocity and acceleration of the motor:

$$\dot{\theta}_m = \frac{\dot{\Gamma}}{c}; \quad \ddot{\theta}_m = \frac{\ddot{\Gamma}}{c}$$

and by substituting these expressions in (7), the new expression for the dynamic model of the complete system is:

$$A_1 c u_c = \dddot{\Gamma} + B_1 \ddot{\Gamma} + \xi_1 \tag{17}$$

where $\xi_1 = c\xi_0$ is an input disturbance to the system.

2.2 Rigid arm

The rigid arm is also actuated by a DC motor and thus, we can consider the rigid arm dynamics as that dynamics of a DC motor in which the complete inertia of the system is the sum of the motor inertia and the inertia of the rigid arm (considering also the inertia of the flexible finger gripper). Taking this into account, we can model the dynamics of the rigid arm as:

$$k_2 u_{c_2} = J_2 \ddot{\hat{\theta}}_{m_2} + \nu_2 \dot{\hat{\theta}}_{m_2} + \hat{\Gamma}_{Coul_2} \tag{18}$$

where k_2 is a motor constant, u_{c_2} is the voltage supplied to the servo-amplifier, J_2 is the motor inertia plus the inertia of the rigid arm, ν_2 is the viscous friction of the motor, $\hat{\Gamma}_{Coul_2}$ is the unknown Coulomb friction torque and $\hat{\theta}_{m_2}$ is the angular position of the motor. By dividing the two terms of (18) by the reduction ratio of the motor gear n_2 and making $A_2 = \frac{k_2}{J_2 n_2}$, $B_2 = \frac{\nu_2}{J_2}$ and $\xi_2 = \hat{\Gamma}_{Coul_2}/(n_2 J_2)$. We obtain:

$$A_2 u_{c_2} = \ddot{\theta}_{m_2} + B_2 \dot{\theta}_{m_2} + \xi_2 \tag{19}$$

where $\ddot{\theta}_{m_2} = \frac{\ddot{\hat{\theta}}_{m_2}}{n_2}$ and $\dot{\theta}_{m_2} = \frac{\dot{\hat{\theta}}_{m_2}}{n_2}$.

3. FEEDBACK CONTROLLER DESIGN

3.1 Second Order Model

Consider the following generalized second order system:

$$\rho_1 x = \ddot{y} + \rho_2 \dot{y} + \xi \tag{20}$$

where ρ_1 and ρ_2 are the system gains, x is the input to the system, y is the output from the system and ξ is a constant perturbation. The controller to be designed will be robust with respect the constant perturbation ξ. Therefore, the transfer function of the system is written as:

$$G(s) = \frac{Y(s)}{X(s)} = \frac{\rho_1}{s(s + \rho_2)} \tag{21}$$

Our objective is to regulate the output of the system y to track a given smooth reference trajectory $y^*(t)$. Another important prevailing restriction throughout our treatment of the problem is our desire *not* to measure, or compute on the basis of samplings, bounded derivatives of the system output y.

3.2 Generalized Proportional Integral Controller

Consider the model given in (20). With some rearrangements, the perturbed system can be written as follows,

$$\ddot{y} = \rho_1 x - \rho_2 \dot{y} - \xi \tag{22}$$

The unperturbed system is flat with flat output given by y. (See Fliess et al. (1995) and Sira-Ramírez and Agrawal (2004)). Clearly, if an open loop control input $x^*(t)$ exists that *ideally* (i.e., under no perturbation inputs) achieves the tracking of y for suitable initial conditions, this must satisfy the second order dynamics of the unperturbed system:

$$\ddot{y}^*(t) = \rho_1 x^*(t) - \rho_2 \dot{y}^*(t) \tag{23}$$

So the nominal control input is computed from the flatness relation,

$$x^*(t) = \frac{1}{\rho_1}\ddot{y}^*(t) + \frac{\rho_2}{\rho_1}\dot{y}^*(t) \tag{24}$$

Given that the system is affected by a constant input, the controller for the system should thus include a double integral compensation action which is capable of overcoming ramp tracking errors. The ramp error is mainly due to the integral angular velocity reconstructor, performed in the presence of constant, or piece-wise constant, perturbations. The integral reconstructor is hidden in the GPI control scheme. Subtracting (23) from (22) an expression in terms of the error in the system is obtained:

$$\ddot{e}_y = \rho_1 e_x - \rho_2 \dot{e}_y - \xi \tag{25}$$

where $e_y = y - y^*(t)$ and $e_x = x - x^*(t)$.

We then propose the following feedback controller:

$$\rho_1 e_x = \rho_2 \dot{e}_y + \left\{ -\lambda_3 \dot{e}_y - \lambda_2 e_y - \lambda_1 \int_0^t e_y(\sigma) d\sigma - \lambda_0 \int_0^t \int_0^{\sigma_1} e_y(\sigma_2) d\sigma_2 d\sigma_1 \right\} \quad (26)$$

By substituting the previous equation (26) in (25) we obtain an expression for the closed loop system, which is evidently represented by an integro-differential equation for the output tracking error $e_y = y - y(t)^*$ as an exponentially stable equilibrium point. The closed loop tracking error e_y evolves governed by,

$$\ddot{e}_y + \lambda_3 \dot{e}_y + \lambda_2 e_y + \lambda_1 \int_0^t e_y(\sigma) d\sigma + \lambda_0 \int_0^t \int_0^{\sigma_1} e_y(\sigma_2) d\sigma_2 d\sigma_1 = 0 \quad (27)$$

The characteristic polynomial associated with this equation is easily shown to be

$$p(s) = s^4 + \lambda_3 s^3 + \lambda_2 s^2 + \lambda_1 s + \lambda_0 = 0 \quad (28)$$

Thus, the design problem is reduced to an appropriate choice of feedback controller gains so as to make the above polynomial Hurwitz.

The signal $\dot{e}_y$ needed in the controller is, unfortunately, not available. We resort to an integral reconstructor of such a signal in order to avoid tracking error velocity measurements. We propose an *integral reconstructor* for the angular velocity error signal $\dot{e}_y$ (See Marquez et al. (2000)). We proceed by integrating the expression (25) just once.

$$\dot{e}_y(t) - \dot{e}_y(0) = \rho_1 \int_0^t e_x(\sigma) d\sigma - \rho_2 \left[e_y(t) - e_y(0) \right] - \xi\, t \quad (29)$$

The integral reconstructor based estimated error velocity $[\dot{e}_{\theta_m}]_e$ is proposed to be of the following form:

$$[\dot{e}_y]_e = \rho_1 \int_0^t e_x(\sigma) d\sigma - \rho_2 e_y(t) \quad (30)$$

The proposed estimate of the system output first derivative above clearly exhibits a structural error of the *ramp* type. The integral reconstructor neglects the effects of, possibly nonzero, initial conditions $\dot{e}_y(0)$ and $e_y(0)$ as well as the effects of a constant perturbation represented by ξ and resulting in a ramp signal error for the angular velocity estimate. This growing error is classically compensated by an iterated tracking error integral action. It is easy to verify that the use of the integral reconstructor does not change the closed loop features of the proposed controller.However, the design gains $\{\lambda_3, \lambda_2, \lambda_1, \lambda_0\}$ need to be more carefully computed when the integral reconstructor is used. The integral reconstructor expression for $\dot{e}_y$ (30) is substituted into the proposed controller (26) and, after some rearrangements the compensator, based on the integral reconstructor and *GPI* is of the form,

$$x = x^*(t) + \left[\frac{\alpha_2 s^2 + \alpha_1 s + \alpha_0}{s(s+\alpha_3)} \right] (y^*(t) - y) \quad (31)$$

with the gains $\alpha_3 = \lambda_3 - \rho_2, \alpha_2 = (\rho_2(\rho_2 - \lambda_3) + \lambda_2)/\rho_1, \alpha_1 = \lambda_1/\rho_1, \alpha_0 = \lambda_0/\rho_1$.

The stability condition on the closed loop expression $(1 + G(s)H(s))$ leads to the following characteristic polynomial,

$$s^4 + (\alpha_3 + \rho_2)s^3 + (\alpha_3\rho_2 + \alpha_2\rho_1)s^2 + \alpha_1\rho_1 s + \alpha_0\rho_1 = 0 \quad (32)$$

This can equate the corresponding coefficients of the closed loop characteristic polynomial (32) with those of a desired fourth order Hurwitz polynomial,

$$p(s) = s^4 + \lambda_3^* s^3 + \lambda_2^* s^2 + \lambda_1^* s + \lambda_0^* = 0 \quad (33)$$

Bearing this in mind, we can choose to place all the closed loop poles at a certain real value, using the following desired polynomial expression,

$$(s+p)^4 = s^4 + 4ps^3 + 6p^2 s^2 + 4p^3 s + p^4 = 0 \quad (34)$$

where the parameter p represents the common location of all the closed loop poles, being this strictly positive. By identifying the corresponding terms of the equations (34) and (32), the parameters $\{\lambda_3, \lambda_2, \lambda_1, \lambda_0\}$ may be uniquely obtained.

Torque Control – The system to control the torque is given by the expression in (17). By comparing this equation with that of (20) the following equivalences are obtained: the equivalences between the two expressions are $A_1 \cdot c = \rho_1$, $B_1 = \rho_2$, $u_c = x$, $\Gamma = y$ and $\xi_1 = \xi$. Thus, the torque controller (see (31)) is designed as

$$u_c = u_c^*(t) + \left[\frac{\alpha_2 s^2 + \alpha_1 s + \alpha_0}{s(s+\alpha_3)} \right] (\Gamma^*(t) - \Gamma) \quad (35)$$

with the gains $\alpha_3 = \lambda_3 - B_1$, $\alpha_2 = (B_1(B_1 - k_3) + \lambda_2)/(A_1 c)$, $\alpha_1 = \lambda_1/(A_1 c)$, $\alpha_0 = \lambda_0/(A_1 c)$. On the other hand, The nominal control input (see (24)) is computed as

$$u_c^*(t) = \frac{1}{A_1 c} \ddot{\Gamma}^*(t) + \frac{B_1}{A_1 c} \dot{\Gamma}^*(t) \quad (36)$$

The impact detection follows the next equation:

$$|\Gamma^*(t) - \Gamma| > \mu \quad (37)$$

where μ is a small value selected by the designer.

Position Control – The system to control the position is given by the expression in (19). By comparing this equation with that used in (20) we obtain that the equivalences between the two expressions are $A_2 = \rho_1$, $B_2 = \rho_2$, $u_{c_2} = x$, $\theta_{m_2} = y$ and $\xi_2 = \xi$. The position controller (see (31)) is designed as

$$u_{c_2} = u_{c_2}^*(t) + \left[\frac{\alpha_2 s^2 + \alpha_1 s + \alpha_0}{s(s+\alpha_3)} \right] (\theta_{m_2}^*(t) - \theta_{m_2}) \quad (38)$$

with the gains $\alpha_3 = \lambda_3 - B_2, \alpha_2 = (B_2(B_2 - \lambda_3) + \lambda_2)/A_2, \alpha_1 = \lambda_1/A_2, \alpha_0 = \lambda_0/A_2$. The nominal control input (see (24)) is computed as

$$u_{c_2}^*(t) = \frac{1}{A_2} \ddot{\theta}_{m_2}^*(t) + \frac{B_2}{A_2} \dot{\theta}_{m_2}^*(t) \quad (39)$$

4. EXPERIMENTAL RESULTS

4.1 Experimental Setup Description

Flexible finger gripper setup – The flexible finger is a rectangular sheet made of spring steel with width 1 $[cm]$, length 7 $[cm]$ and thickness 0.55 $[mm]$. One end of the flexible finger is clamped to a DC motor C-6065, which has a reduction ratio $n = 100$. The motor is fixed to the rigid arm. A servoamplifier supplies the DC motor of the flexible finger. This saturates at voltages -0.3 $[V]$ and 0.3 $[V]$. The parameters used for the torque control were estimated as done in Mamani et al. (2007). They are: the product $A_1 c = 17$ $[N^2/(V \cdot kg)]$, $B_1 = 0.8$ $[N \cdot s/(kg \cdot m)]$ and $\xi_1 = 2.02$ $[N^2/kg]$ (the voltage applied to the motor to overcome the Coulomb's friction is $\xi_1/A_1 c = 0.12$ $[V]$). The sensor system is only integrated by a pair of strain gauges with

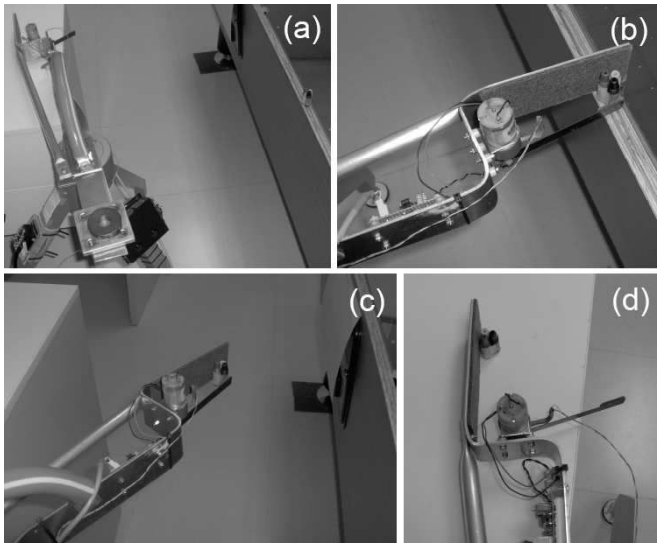

Fig. 5. (a) Initial position of the robot. (b) Grasping the object. (c) Moving the object. (d) Releasing the object.

gage factor 2.16 and resistance 120.2 $[\Omega]$. Finally, the sample time is 2 $[ms]$.

Rigid arm setup – The used experimental platform is constituted by a three legged metallic structure to support an Harmonic Drive mini servo DC motor RH-8D-6006-E050AL-SP(N) which has a reduction ratio characterized by $n = 50$. The frame makes possible the stably and free rotation of the motor in the horizontal plane around the vertical axis of the platform. The parameter values A_2 and B_2 of the transfer function of the rigid arm DC motor in (21) were estimated with the method explained in Mamani et al. (2007), and the values are: $A_2 = 13\ [N/(V \cdot kg \cdot m)]$, $B_2 = 2.8\ [N \cdot s/(kg \cdot m)]$ and $\xi_2 = 7.41\ [N/(kg \cdot m)]$.The rigid arm is made of aluminium and supports the flexible finger gripper. The servoamplifier accepts control inputs from the computer in the range of $[-10, 10]\ [V]$. The sensor system is integrated by an encoder embedded in the motor which allows us to know the rigid arm position with a precision of $7 \cdot 10^{-5}\ [rad]$. Fig.5 depicts photographs of the robot in an experiment of grasping and moving an object in real time.

4.2 Controllers Design

For the flexible finger gripper torque controller the poles are placed at -30 in the real axis. The torque controller in (35) is designed with the gains $\alpha_3 = 119.20, \alpha_2 = 312.04, \alpha_1 = 6.35 \cdot 10^3, \alpha_0 = 4.76 \cdot 10^4$. The nominal control input in (36)is computed as $u_c^*(t) = 0.06\ddot{\Gamma}^*(t) + 0.05\dot{\Gamma}^*(t)$.

For the rigid arm position controller the poles are placed at a reasonable location of the negative real axis:-90. The position controller for the rigid arm in (38) is designed with the gains $\alpha_3 = 357.20, \alpha_2 = 3.66 \cdot 10^3, \alpha_1 = 2.24 \cdot 10^5, \alpha_0 = 5.05 \cdot 10^6$. The nominal control input in (39) is computed as $u_{c_2}^*(t) = 0.08\ddot{\theta}_m^*(t) + 0.22\dot{\theta}_m^*(t)$.

4.3 Results

In the platform, the rigid arm position control and the flexible finger gripper torque control are combined to be applied in grasping and moving objects from one location to other.

Rigid arm position control – Fig. 6 depicts an scheme of the closed loop position controller for the rigid arm. The rigid arm is initially placed in a defined location which we take as reference, it is 0 $[rad]$. After, the arm is positioned in the location where the object to be moved is placed, it is 1.3 $[rad]$, by following a reference trajectory during 7 $[s]$. The trajectory tracking is depicted in Fig.8(a). When the rigid arm arrives to this position the block *I.P* (Initial Position), which is a digital switch that indicates the initial position of the rigid robot (see Fig. 6) is turned on at high level, this item will be used in the torque control of the gripper. The rigid arm maintains the position during 5 $[s]$ which is the time in which the object is grasped with the flexible finger gripper. In due course, at time $t = 12\ [s]$ the rigid arm starts a new trajectory to be positioned in the initial location seven seconds later and the block *I.P* is turned off at low level. The experiment finishes at time $t = 20\ [s]$ and the block *F.P* (Final Position), which is a digital switch that indicates the final position of the rigid robot and which is turned on at high level (see Fig.6). Note that the two trajectories, reference $\theta_{m_2}^*$ and rigid arm position θ_{m_2}, are superimposed. Fig.8(b) depicts the trajectory tracking error $\theta_{m_2}^* - \theta_{m_2}$ which is very small, $10^{-3}\ [rad]$ order. The control input voltage to the rigid arm motor is represented in Fig.8(c). The control effort is small and the voltage signal never exceeds the values 10 $[V]$ and $-10\ [V]$, therefore, the amplifier never saturates.

Flexible finger gripper torque control – Fig.7 depicts the closed loop feedback torque control for the flexible finger gripper. While the rigid arm is being positioned to the place where the object is located, the flexible finger gripper is not being controlled. Nevertheless a reference torque trajectory Γ^* is generated since the start with an amplitud 0.01 $[Nm]$ (see Fig.8(d)) because the time at which the object is detected is not known, thus when the object is detected, the controller makes the flexible finger to track this trajectory to grasp the object with a small force. Obviously, the torque is null until the object is detected, and appears a small error until $t = 7\ [s]$ (see Fig.8(e), which illustrates the tracking error in the torque control system). At this time $t = 7\ [s]$ the rigid arm is positioned in 1.3 $[rad]$ very near to the object. The block *I.P* (see Fig.7) is turned on at high level, this causes that the switch is connected at position 1 (see Fig.7) and this position is

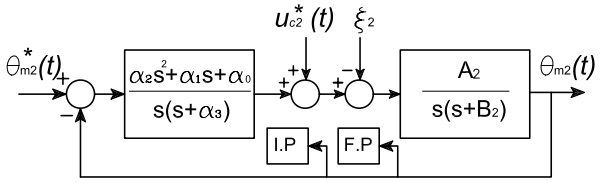

Fig. 6. Closed loop feedback position control for the rigid arm.

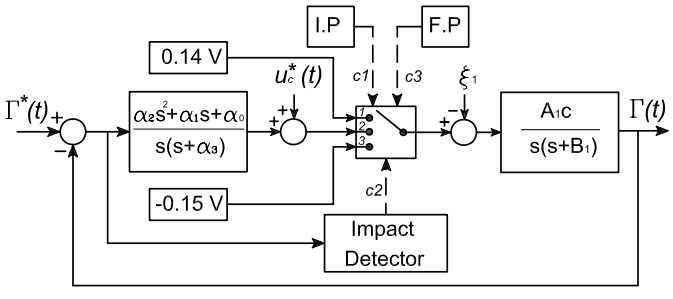

Fig. 7. Closed loop torque control scheme.

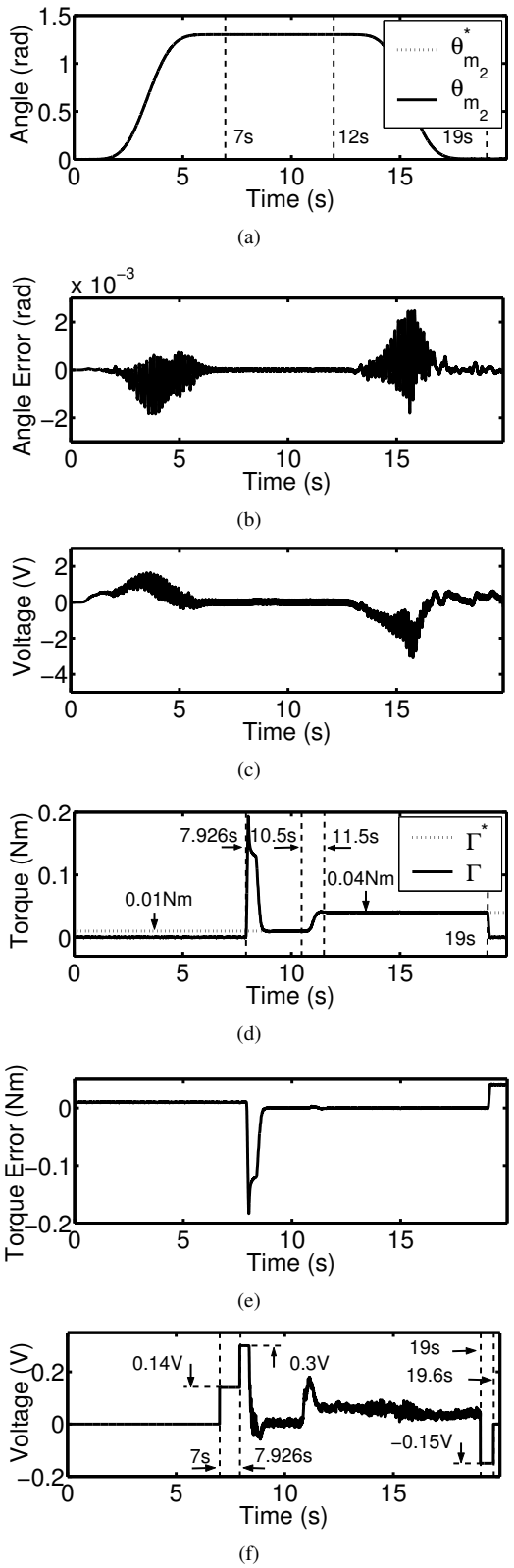

Fig. 8. (a) Trajectory tracking of the rigid dynamics position. (b) Trajectory tracking error of the rigid dynamics position $\theta^*_{m_2} - \theta_{m_2}$. (c) Control input voltage to the rigid arm DC motor. (d) Force trajectory tracking of the flexible finger gripper. (e) Force trajectory tracking error of the flexible finger gripper. (f) Control input voltage to the dc motor of the flexible finger gripper.

maintained until input c_2 of the switch changes from low level to high level. A positive voltage of 0.14 $[V]$ (any other voltage higher than $\xi_1/A_1c = 0.12[V]$ is also available) is then applied to the flexible finger gripper motor. This voltage produces a slow movement of the finger gripper, which brings near the object carefully. At time $t = 7.926$ $[s]$ the flexible finger gripper impacts with the object and this impact is instantaneously detected with the impact detector (see (37)) when $|\Gamma^*(t) - \Gamma| > 0.12$, whose output is turned on at high level, this causes that the switch connects at position 2 and maintain it until the input c_3 of the switch changes from low to high level. The controller starts and calculates a voltage which saturates the flexible finger gripper amplifier, which saturates at 0.3 V during a very small period of time. Later, the gripper perfectly tracks the reference trajectory of 0.01 $[Nm]$. At this instant, a new reference trajectory is generated as a Bezier's eight order polynomial which begins at 0.01 $[Nm]$ and finishes at 0.04 $[Nm]$. The time of this trajectory is 1 $[s]$. The gripper maintains the torque determined by the reference trajectory while the rigid arm is moving to the initial position (see Fig.8(a) and Fig.8(d)). Note that the tracking error is null since the controller reduces the impact error until time $t = 19$ $[s]$ when the rigid arm arrives to the final location and the block *F.P* (see Fig.6 and Fig.7) changes the switch input c_3 from low to high level. The switch (see Fig.7) connects at position 3. From this instant the controller is turned off and a voltage of -0.15 $[V]$ (Note $\xi_1/A_1c = -0.12[V]$) during 0.6 $[s]$ is included in the flexible finger gripper motor to place the finger gripper in the initial position. The object is placed in the location desired. At this moment, the robot is prepared to initiate another movement, thus, the block *F.P* changes to low level and the switch opens the circuit until the input c_1 changes to high level again.

5. CONCLUSIONS

A GPI controller is proposed to control the torque of a flexible finger gripper placed at the tip of a rigid arm whose position is also controlled. This robot can grasp and move objects from a place to other. In many articles of the literature the control of robots has been approached from classical control schemes, such as PD and PID. Generally speaking, those classical control schemes yield good results; nevertheless, they do require the estimation, or on line computation, of bounded derivatives of the measured signals. These signals are customarily quite noisy and the use of low pass filters become necessary to smooth them causing the well known delays that affect the performance and accuracy of the tracking maneuver. We have proven that this king of controllers proposed perform suitably for both rigid and flexible robots and the estimation and computation of bounded derivatives of the measured signals is not really necessary. The feedback control of this kind of robotic systems in which the motion is driven by DC motors usually involve an estimation, and subsequent compensation, of the nonlinear friction effects. In many cases, this torque is difficult to estimate because of some additional strong non linearities in the friction phenomena, yielding additional parameters to be estimated. The GPI feedback torque control scheme is quite robust with respect the torque produced by the friction term and its estimation is not really necessary. The position control only requires the measure of an encoder and the torque control only requires the measure of a pair of strain gages placed at the root of the flexible estructure. This configuration eliminates the danger of damaging the torque-force sensors because these are never in

contact with the object to be impacted. Experimental results provide accurate results.

REFERENCES

J. Becedas, J. Trapero, H. Sira-Ramírez, and V. Feliu. Fast identification method to control a flexible manipulator with parameters uncertainties. In *IEEE International Conference on Robobotics and Automation*, 2007.

A. Bicchi. Hands for dexterous manipulation and robust grasping: a difficult road toward simplicity. *IEEE Transactions on Robotics and Automation*, 16(6):652–662, 2000.

B.V. Chapnik, G.R. Heppler, and J.D. Aplevich. Controlling the impact response of a one-link flexible robotic arm. *IEEE Transactions on Robotics and Automation*, 9(3):346–351, 1993.

B.C. Chiou and M. Shahinpoor. Dynamics stability analysis of a one-link force-controlled flexible manipulator. *Journal of Robotic Systems*, 5(5):443–451, 1988.

J.W. Choi and N.I. Cho. Suppression of narrow-band interference in DS-spread spectrum systems using adaptive IIR notch filter. *Signal Processing*, 82(12):2003–2013, 2002.

D. Erickson, M. Weber, and I. Sharf. Contact stiffness and damping estimation for robotic systems. *International Journal of Robotics Research*, 22(1):41–57, 2003.

V. Feliu and F. Ramos. Straing gauge based control of single-link flexible very light weight robots robust to payload changes. *Mechatronics*, 15:547–571, 2005.

M. Fliess, J. Levine, P. Martin, and P. Rouchon. Flatness and defect of nonlinear systems: Introductory theory and examples. *International Journal of Control*, 61:1327–1361, 1995.

T. Fukuda, N. Kitamura, and K. Tanie. Flexible handling by gripper with consideration of characteristics of objects. In *IEEE Proceedings on Robotics and Automation*, volume 3, 1986.

G. Gilardi and I. Sharf. Literature survey of contact dynamics modelling. *Mechanical and Machine Theory.*, 37:1213–1239, 2002.

P. Gorce and J.G. Fontaine. Design methodology approach for flexible grippers. *Journal of Intelligent and Robotic Systems*, 15(3):307–328, 1996.

J. Y Lew and W. J. Book. Hybrid control of flexible manipulators with multiple contact. *IEEE International Conference on Robotics and Automation*, pages 242–247, 1993.

G. Mamani, J. Becedas, V. Feliu, and H. Sira-Ramírez. Open-loop algebraic identification method for a dc motor. In *IFAC/ACPA/IEEE European Control Conference*, 2007.

R. Marquez, E. Delaleau, and M. Fliess. Commande par pid généralisé d'un moteur électrique sans capteur mecanique. In *Premiére Conférence Internationale Francophone d'Automatique*, 2000.

F. Matsuno and S. Kasai. Modeling and robust force control of constrained one-link flexible arms. *Journal of Robotic Systems*, 15(8):447–464, 1998.

L. Shi and M. Trabia. Comparison of distributed pd-like and importancebased fuzzy logic controllers for a two-link rigid-flexible manipulator. *Journal of Vibration and Control.*, 11: 723–747, 2005.

K.B. Shimoga. Robot grasp synthesis algorithms: a survey. *International Journal of Robotics Research*, 15:230–266, 1996.

H. Sira-Ramírez and S. Agrawal. *Differentially flat systems*. Marcel Dekker, 2004.

M. Tanaka, S. Chonan, and Z. Jiang. Force control of a flexible finger with distributed sensors and piezoelectric actuators. *Journal of Intelligent Material Systems and Structures.*, 7(3): 301–306, 1996.

L. Tian, J. Wang, and Z. Mao. Constrained motion control of flexible robot manipulators based on recurrent neural networks. *IEEE Transaction on Systems, Man and Cybernetics.*, 34:1541–1552, 2004.

T. Yoshikawa, K. Harada, and A. Matsumoto. Hybrid position/force control of flexible-macro/rigid-micro manipulator systems. *IEEE Transactions on Robotics and Automation.*, 12(4):633–640, 1996.